

**Increased Melting of Marine-Terminating Glaciers by  
Sediment-Laden Plumes**

**C. D. McConnochie<sup>1</sup>and C. Cenedese<sup>2</sup>**

<sup>4</sup><sup>1</sup>Department of Civil and Natural Resources Engineering, University of Canterbury

<sup>5</sup><sup>2</sup>Physical Oceanography Department, Woods Hole Oceanographic Institution

**6 Key Points:**

- <sup>7</sup> • Submarine melting of an ice face can be increased by the presence of sediment in  
<sup>8</sup> a subglacial discharge plume
- <sup>9</sup> • The increased melting is due to increased entrainment into the plume, showing  
<sup>10</sup> a direct link between entrainment and melting
- <sup>11</sup> • A modification to a common submarine ice melting parameterization is proposed  
<sup>12</sup> which accounts for the link between entrainment and melting

13      **Abstract**

14      This paper summarizes the results of the first investigation into the effect of particle-  
 15      laden plumes on glacier melting using laboratory experiments. We find that the melt rate,  
 16      when the ice is exposed to a particle-laden plume, can be increased by up to 60% com-  
 17      pared to when the ice is exposed to an equivalent plume without particles. The increased  
 18      melt rate is linked to increased entrainment into the turbulent plume, demonstrating a  
 19      link between turbulent entrainment and the melt rate of the ice face. We use this link  
 20      to propose a modification to the commonly used ‘three-equation model’ that explicitly  
 21      accounts for variations in entrainment rates.

22      **Plain Language Summary**

23      Ice loss from the Greenland ice sheet is more rapid in locations where fresh water  
 24      is released at the base of marine terminating glaciers. The fresh water forms a buoyant  
 25      plume that rises vertically next to the ice face. Previous observations of these plumes  
 26      have shown that they can contain significant concentrations of suspended sediment. We  
 27      show, using laboratory experiments, that the melt rate of a vertical ice face is increased  
 28      by up to 60% by the presence of suspended particles in the vertically rising plume. This  
 29      observation suggests that the effect of such plumes could be larger than current mod-  
 30      elling studies predict. Finally, we suggest an adjustment to those models such that the  
 31      effects of sediment-laden plumes can be fully accounted for.

32      **1 Introduction**

33      Ice loss from the Greenland Ice Sheet is currently a major contributor to global sea  
 34      level rise. Approximately half of this ice loss is due to the calving of icebergs with the  
 35      remainder due to direct melting of marine-terminating glaciers into the ocean (Rignot  
 36      et al., 2013). Although the melt rate has been increasing over recent years (Pritchard  
 37      et al., 2009), there remains a large uncertainty in predictions of future melt rates. In-  
 38      creasing our understanding of glacier melt rates and associated drivers, enables better  
 39      predictions of future sea level rise and better planning decisions to be made.

40      For both calving of icebergs and direct melting of the ice sheet, the interaction be-  
 41      tween the ocean and the ice face is crucial. The ocean provides a source of heat and salt  
 42      to the ice, the transport of which directly determines the melt rate of the ice face (Jenkins,

43 2011; Kerr & McConnochie, 2015). However, the transport process itself is highly com-  
 44 plex and involves both relatively large-scale turbulent processes and small-scale molec-  
 45 ular processes.

46 A commonly used numerical parameterization developed to predict the melt rate  
 47 of an ice face based on the bulk temperature, salinity and velocity close to the ice is known  
 48 as the ‘three-equation model’ (e.g. Jenkins, 2011). Both the turbulent and molecular trans-  
 49 port processes are parameterized by constant transfer coefficients to give the flux of heat  
 50 and salt to the ice face. These transfer coefficients will hereafter be referred to collec-  
 51 tively as  $\Gamma_{T,S}$ .

52 Due to the relatively warm air temperatures in Greenland over summer, a signif-  
 53 icant amount of surface melting of the ice sheet occurs. The surface meltwater sinks to  
 54 the base of the ice sheet and flows beneath glaciers to the grounding line — the loca-  
 55 tion where a glacier becomes afloat (Nienow, 2017). At the grounding line, the meltwa-  
 56 ter is released into the ocean and forms a highly vigorous turbulent plume that rises along  
 57 the ice face (Fried et al., 2015; Straneo & Cenedese, 2015). The dynamics of subglacial  
 58 plumes have received a large amount of attention over recent years as they are often as-  
 59 sociated with elevated melt rates (see Straneo & Cenedese, 2015).

60 As the surface meltwater flows beneath the ice sheet it can erode significant amounts  
 61 of sediment. As a result, subglacial plumes contain high sediment concentrations and can  
 62 often be observed from surface photographs when they reach the surface (Mankoff et al.,  
 63 2016). Recent experimental work has shown that the entrainment of ambient water into  
 64 an axisymmetric turbulent plume is increased by up to 40% when the plume contains  
 65 suspended dense sediment (McConnochie et al., 2021). Given that the transport of heat  
 66 and salt to the ice face occurs mainly by entrainment of ambient fluid into the subglacial  
 67 plumes, it could be expected that the sediment contained in subglacial plumes would en-  
 68 hance the melt rate of the glacier. In contrast, the three-equation model would predict  
 69 reduced melt rates as higher rates of entrainment will cause the plume to decelerate more  
 70 rapidly and reduce the parameterized transport of heat and salt. This contradiction leaves  
 71 it unclear how the suspended sediment carried in subglacial plumes will affect the melt  
 72 rate of a glacier face and how such effects should be included in numerical models.

73 In this paper we present laboratory experiments of a vertical ice face melting in  
 74 contact with a particle-laden plume. Section 2 contains a description of the experimen-

75 tal apparatus and procedure. Experimental results are presented in Section 3 before a  
 76 discussion of the implications for modelling ice-ocean interactions is provided in Section 4.

77 **2 Methods**

78 Experiments were conducted in a glass walled tank that was 150 cm long, 15 cm  
 79 wide and 30 cm high and is shown schematically in Figure 1a. The tank was stored in  
 80 a temperature controlled room that was kept at approximately 3 °C. The tank was ini-  
 81 tially filled to a depth of 25 cm with oceanic salt water that had been left in the room  
 82 to thermally equilibrate for at least 24 hours prior to the experiment.

83 In all experiments, the ambient fluid temperature and salinity were  $3.2 \pm 0.2$  °C  
 84 and  $3.35 \pm 0.05$  wt.%, respectively. The plume fluid is supplied to the base of the ice block  
 85 with a flow rate  $Q_s$  of  $6.0 \pm 0.1 \text{ cm}^3 \text{ s}^{-1}$  and fluid is removed from the tank at the same  
 86 flow rate from the opposite end. The buoyancy flux due to the subglacial discharge is  
 87 approximately 25 times that due to the melting of the ice face such that the buoyancy  
 88 flux of the plume can be assumed to be constant with height and dominated by the source  
 89 buoyancy flux (McConnochie & Kerr, 2017a). Particles fall out from the surface current  
 90 (Figure 1) with a settling velocity  $v_s$  which is significantly smaller than the velocity of  
 91 the rising plume next to the ice.

92 The ice used in the experiments was made from fresh water with a small amount  
 93 of blue food dye added for visualization. The fresh water was left at room temperature  
 94 for at least 48 hours prior to being frozen so that the ice was free of air bubbles. The  
 95 water was frozen in a mould in a freezer for at least 48 hours until it came to a uniform  
 96 temperature. The mould was constructed such that the width of the ice block was slightly  
 97 smaller than the width of the tank so the ice block could be smoothly placed in, and re-  
 98 moved from, the tank. Although this resulted in a very thin layer of fluid being trapped  
 99 between the ice block and the tank wall, this did not appear to result in further convec-  
 100 tion and the melting against the sides of the tank was negligible. Prior to the experi-  
 101 ment the ice was removed from the mould and placed in the temperature controlled room  
 102 for 90 minutes. During this time the ice began to warm up but didn't start melting which  
 103 ensured that almost all of the heat flux to the ice during an experiment resulted in melt-  
 104 ing of the ice rather than warming, and that the measured melt rate was approximately

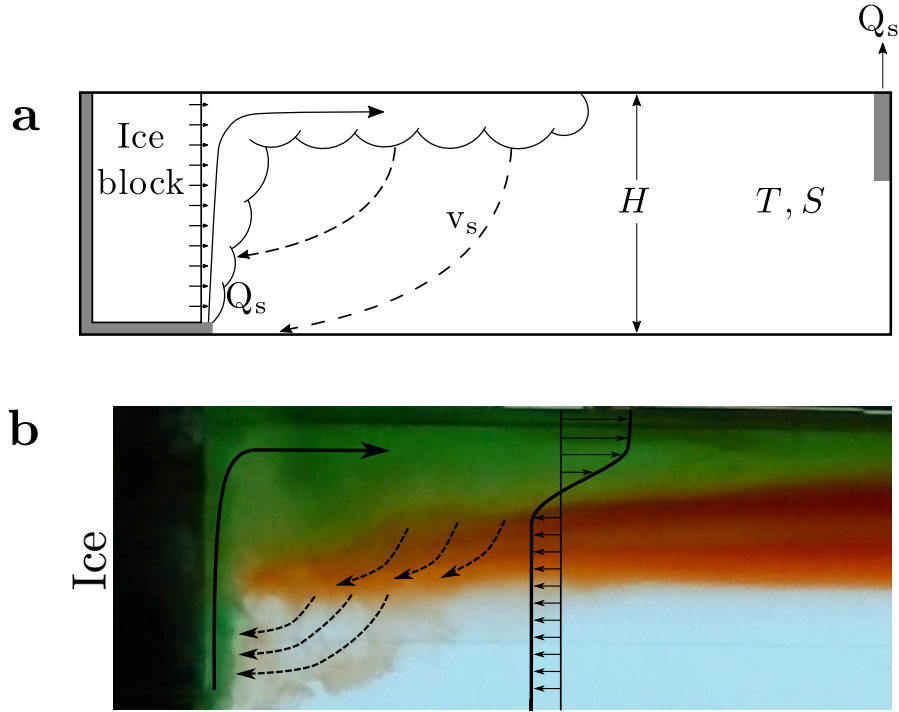


**Figure 1.** a) A schematic of the tank used in the experiments. The tank is filled to a depth  $H$  with ambient fluid of temperature  $T$  and salinity  $S$  and an ice block is placed against one end wall. The plume fluid is supplied to the base of the ice block with a flow rate  $Q_s$  and drawn out of the tank with the same flow rate from the opposite side. Particles fall from the surface buoyant current with a settling velocity  $v_s$  which is significantly smaller than the velocity of the rising plume next to the ice.

b) A photograph taken from a qualitative experiment of the top-left section of the tank. The source fluid was dyed green and a layer of fluid close to the surface at the start of the experiment was dyed red. The light red region in the bottom half of the tank indicates particles settling and being drawn back to the ice face due to turbulent entrainment. The light red color is caused by the transport of some ambient water by the settling particles.

105 proportional to the total heat flux to the ice. Immediately before placing the ice in the  
106 tank it was dried and weighed on a scale.

107 During an experiment, a fresh water line plume was produced at the base of the  
108 ice block. The line plume was produced from an array of ten point sources equally spaced  
109 across the width of the tank. Each source was designed to generate a turbulent plume  
110 at the exit location (Kaye & Linden, 2004) and the individual plumes quickly merged  
111 to form a line plume. The melt rate of the ice block was observed to be higher above the  
112 source locations along the bottom 1–2 cm of the ice block. Above this height the melt  
113 rate was spatially uniform, suggesting that the velocity of the plume was also spatially  
114 uniform — i.e. that the plume was two-dimensional.

115 The plume source fluid was fresh water that had been stored in the cold room for  
116 24 hours. Prior to the experiment small ice cubes were added to the source fluid to re-  
117 duce the temperature of the fluid to between 0.5 and 1.0 °C. The exact temperature of  
118 the source fluid was measured to within  $\pm 0.1$  °C with an alcohol thermometer immedi-  
119 ately prior to an experiment. Immediately before an experiment the ice cubes were re-  
120 moved, food dye was added to the fresh water for visualization and the desired mass of  
121 particles was added to the fluid. These particles were kept in suspension during an ex-  
122 periment by continually stirring the source fluid.

123 The particles used were solid glass microspheres with a density of  $2.5 \text{ g/cm}^3$  and  
124 diameters of  $38\text{--}53 \mu\text{m}$ . During an experiment the plume fluid containing the particles  
125 rose vertically along the ice face before spreading as a buoyant surface current. As the  
126 plume fluid spread along the surface, particles settled from the surface current and were  
127 drawn back towards the ice face due to the entrainment of ambient fluid into the plume  
128 (Figure 1).

129 Each experiment was run for approximately 5 minutes. After this time, the ice block  
130 face started to retreat behind the position of the source and the height where the plume  
131 became attached to the ice face began to shift upwards. At the conclusion of an exper-  
132 iment the ice was removed from the tank, dried, and weighed. The loss of mass during  
133 an experiment was used to estimate the melt rate based on a density of ice of  $0.92 \text{ g cm}^{-3}$   
134 and assuming that the melting was uniformly distributed over the ice face that was ex-  
135 posed to the particle-laden plume.

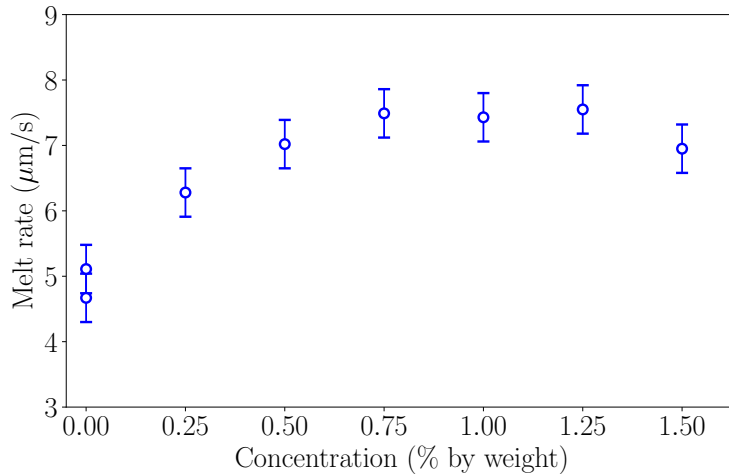


**Figure 2.** Measured melt rate as a function of sediment concentration by weight.

136       Figure 1b shows a photo from a qualitative experiment. A freshwater subglacial  
 137       line plume (dyed green) was produced at the base of an ice block (dyed blue) which rose  
 138       vertically and spread horizontally once it reached the free surface. Experiments were car-  
 139       ried out with different concentrations of particles added to the subglacial plume. Sim-  
 140       ilarly to the experiments presented in Sutherland et al. (2020), particles are expected to  
 141       settle from the horizontally flowing surface current before being drawn back towards the  
 142       ice face by entrainment of ambient fluid into the plume (dashed lines in Figure 1a and  
 143       b).

### 144       **3 Results**

145       The measured melt rate is shown in Figure 2 as a function of sediment concentra-  
 146       tion by weight. The estimated uncertainty shown in Figure 2 is the difference between  
 147       two repeated experiments without particles. Figure 2 clearly shows that the melt rate  
 148       of the ice block is strongly dependent on the sediment concentration. Furthermore, this  
 149       dependence appears to be complex and non-linear. At low particle concentrations, the  
 150       measured melt rate increases rapidly with the particle concentration until the melt rate  
 151       is approximately 60% larger than that without added particles. However, further increas-  
 152       ing the particle concentration has no effect on the measured melt rate.

153       As in McConnochie et al. (2021), we attempt to understand this non-linear response  
 154       by characterizing the particle concentration by a buoyancy flux ratio,  $P$ . The buoyancy

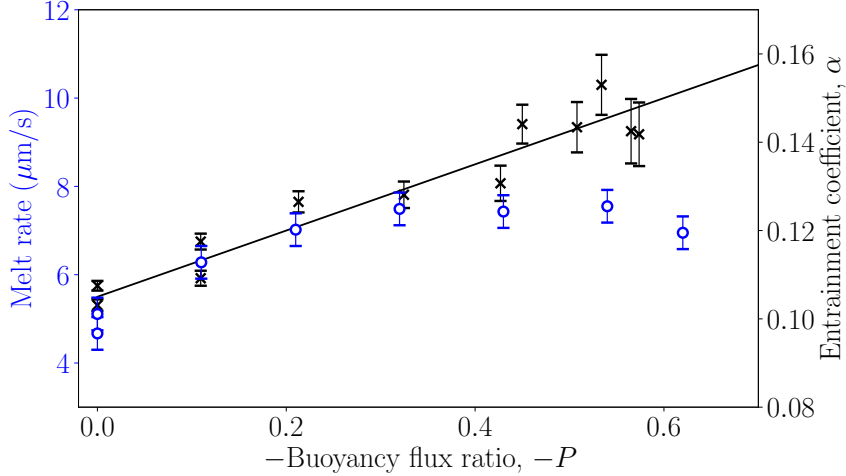


**Figure 3.** Measured melt rate (blue circles, left axis) and the entrainment coefficient estimated by McConnachie et al. (2021) (black crosses, right axis) plotted against the buoyancy flux ratio. Also shown is an empirical fit to the entrainment coefficient (black line, right axis) from McConnachie et al. (2021) given by  $\alpha = 0.105 - 0.75P$ .

flux ratio compares the component of the source buoyancy flux that is due to the particles,  $B_{\text{part}}$ , with the buoyancy flux due to the temperature and salinity induced density differences between the plume and the ambient fluid,  $B_{\text{fluid}}$ :

$$P = \frac{B_{\text{part}}}{B_{\text{fluid}}} \quad (1)$$

Here the buoyancy flux is defined as

$$B = Q_0 g \left( \frac{\rho_a - \rho_0}{\rho_a} \right) \quad (2)$$

where  $Q_0$  is the plume volume flux at the source,  $g$  is the acceleration due to gravity,  $\rho_a$  is the ambient fluid density, and  $\rho_0$  is the source fluid density. The total source buoyancy flux is the given by  $B_{\text{part}} + B_{\text{fluid}}$ , and  $P = 0$  corresponds to a plume with no particles while  $P = -1$  corresponds to a plume where the particle buoyancy is exactly balanced by the fluid buoyancy. Note that  $P \leq 0$  since the buoyancy flux due to the particles is downwards while the buoyancy flux due to fluid density differences is upwards.

On Figure 3 we show the same measurements of melt rate that were shown on Figure 2 but plotted against the buoyancy flux ratio instead of the particle concentration. Estimates of the entrainment coefficient with an empirical fit through the data, both from McConnachie et al. (2021), are also shown on Figure 3. Results from McConnachie et

169 al. (2021) are only shown for those experiments that had a particle size equal to that used  
 170 in the present study. The entrainment coefficient is defined as  $\alpha = U_e/U$ , where  $U_e$  is  
 171 the velocity with which ambient fluid is entrained into the plume and  $U$  is the charac-  
 172 teristic plume velocity (Morton et al., 1956).

173 Figure 3 shows a clear relationship between the melt rate and the entrainment co-  
 174 efficient. McConnochie et al. (2021) suggested that the entrainment coefficient increases  
 175 linearly with the buoyancy ratio. We find that the melt rate also increases linearly with  
 176 the buoyancy ratio, up to some limit where it becomes insensitive to further increases.  
 177 From the data of McConnochie et al. (2021), it remains unclear if the entrainment co-  
 178 efficient also reaches a maximum value, or would do so at larger values of  $-P$ . We note  
 179 that the plume in this study was a two-dimensional line plume whereas that used in McConnochie  
 180 et al. (2021) was an axisymmetric plume. Although we expect the dependence of the en-  
 181 trainment coefficient on the buoyancy flux ratio to be similar, the different geometries  
 182 could explain the difference between the melt rate and the entrainment coefficient at large  
 183 values of  $-P$ .

184 Although the present experiments were conducted with a single buoyancy flux and  
 185 a single particle size, we expect the results to hold provided the particle size is sufficiently  
 186 small, and the buoyancy flux is sufficiently large, that individual particles do not settle  
 187 from the turbulent plume. McConnochie et al. (2021) showed that the entrainment co-  
 188 efficient is only a function of the particle concentration and does not depend on the buoy-  
 189 ancy flux or the particle size (at least within a range of particle sizes). However, as pre-  
 190 viously observed, increasing the source buoyancy flux of the plume will increase the ve-  
 191 locity of the plume and hence the melt rate (McConnochie & Kerr, 2017a). The depen-  
 192 dence of the melt rate on the buoyancy flux is separate from the dependence on the en-  
 193 trainment coefficient illustrated in Figure 3 and is expected to be unchanged with lit-  
 194 tle interaction between the two processes.

## 195 4 Discussion

### 196 4.1 Implications For Modelling the Melt Rate

197 The results of this study show, for the first time, a direct link between the entrain-  
 198 ment of ambient fluid into a turbulent plume and the melting of an ice face. This link  
 199 is not entirely unexpected as both processes involve turbulent transport from the am-

200 bient fluid into the plume. However, the result is also not obvious. Turbulent entrain-  
 201 ment involves the movement of irrotational fluid across a vorticity interface located at  
 202 the edge of a plume. In contrast, melting of the ice face involves scalar transport of heat  
 203 and salt due to both turbulent processes across the plume and molecular processes across  
 204 a small but important laminar sublayer next to the ice face (Wells & Worster, 2008; Mc-  
 205 Connockie & Kerr, 2017b). Given the close link between turbulent entrainment and the  
 206 melt rate of an ice face (Figure 3), it becomes clear that the melt rate should depend on  
 207 all factors that affect turbulent entrainment, not only the presence and concentration  
 208 of suspended sediment. These potentially important factors include the geometry of the  
 209 flow and the nature of the buoyancy source.

210 Current understanding of the effect of subglacial plumes on glacial melting implies  
 211 that subglacial plumes increase the melt rate of an ice face by increasing the flow veloc-  
 212 ity next to the ice. Although this mechanism is undoubtedly important, the direct link  
 213 between entrainment and melting introduces new processes whereby subglacial plumes  
 214 could affect the melt rate of an ice face. The entrainment coefficient of a point source  
 215 plume originating from the base of an ice face is expected to be different to that of a plume  
 216 from a line source (Richardson & Hunt, 2022). Thus, the initial geometry of the subglacial  
 217 discharge will influence the melt rate of an ice face (Cenedese & Gatto, 2016; Slater et al., 2015),  
 218 even in cases where the velocity next to the ice is identical.

219 The entrainment coefficient of a plume adjacent to an ice face will also depend on  
 220 whether the plume buoyancy flux is dominated by that of the subglacial discharge or by  
 221 that due to the release of fresh water due to melting (McConnockie & Kerr, 2017a). Which  
 222 source of buoyancy is dominant will change with height (as increasing amounts of melt-  
 223 water are released) and seasonally (as the subglacial discharge flux changes). Therefore,  
 224 the entrainment coefficient, and hence the melt rate, is expected to vary both season-  
 225 ally and with depth. We note again that the impact on the entrainment coefficient is sep-  
 226 arate from the direct impact that changing the subglacial discharge flux will have on the  
 227 plume velocity.

228 A related question to that asked here is whether the presence of bubbles in a sub-  
 229 glacial plume could have a similar impact on the melt rate as the presence of suspended  
 230 sediment does. These bubbles could plausibly enter the subglacial plume due to gas that  
 231 was initially frozen into the ice being released as it melts. Laboratory experiments have

232 found that bubbles frozen into the ice do not affect the melt rate of the ice (Josberger,  
 233 1980), and this is not expected to change at a geophysical scale. The different behaviour  
 234 with bubbles and solid particles can be explained by previous studies that have shown  
 235 that, provided the rise velocity of the bubbles is smaller than that of the plume, bub-  
 236 ble plumes behave much like single-phase plumes (Mingotti & Woods, 2019). In addi-  
 237 tion, the dependence of the entrainment coefficient on the buoyancy flux ratio shown in  
 238 Figure 3 was not observed when the particle buoyancy and the fluid buoyancy acted in  
 239 the same direction and  $P > 0$  (McConnochie et al., 2021), as would be the case if the  
 240 particles in a subglacial discharge were replaced with bubbles.

#### 241 4.2 Updated Melting Parameterization

242 Currently the three-equation model parameterizes the transport of heat and salt  
 243 through constant transfer coefficients which are multiplied by the flow velocity and a con-  
 244 stant drag coefficient (see Jenkins, 2011). However, the present study shows that it is  
 245 the entrainment velocity, rather than the flow velocity, that governs the transport of heat  
 246 and salt, suggesting that modifications need to be made to the parameterization. We pro-  
 247 pose redefining the scalar transfer coefficients,  $\Gamma_{T,S}$ , to more accurately and explicitly  
 248 represent the two factors that affect the transport of heat and salt to the ice face:

$$\Gamma_{T,S} \equiv \alpha \hat{\Gamma}_{T,S}. \quad (3)$$

249 Here we have separated the traditional transfer coefficients,  $\Gamma_{T,S}$ , into two new compo-  
 250 nents. The first is the entrainment coefficient,  $\alpha$ , and the second is an updated trans-  
 251 fer coefficient,  $\hat{\Gamma}_{T,S}$ , which acts upon the entrainment velocity rather than the flow ve-  
 252 locity:

$$Q_{T,S} = C_D^{1/2} U \Gamma_{T,S} \Delta_{T,S} = C_D^{1/2} \alpha U \hat{\Gamma}_{T,S} \Delta_{T,S}, \quad (4)$$

253 where  $Q_{T,S}$  is the flux of heat or salt,  $C_D$  is the drag coefficient, and  $\Delta_{T,S}$  is the driv-  
 254 ing temperature or salinity difference. The advantage of this new formulation is that it  
 255 explicitly includes the relationship between the transport of heat and salt to the ice face  
 256 and the entrainment coefficient, while still allowing the scalar transport coefficients to  
 257 take constant values.

258 Equation (3) can be easily implemented into the three-equation model and does  
 259 not require the knowledge of additional parameters since the entrainment coefficient is  
 260 typically already used in a coupled plume model to determine the flow velocity (Jenkins,

261 2011). However, it importantly accounts for the fact that the entrainment coefficient will  
 262 have different values in different situations based on the plume source geometry (Cenedese  
 263 & Linden, 2014; Richardson & Hunt, 2022) and sediment concentration (McConnochie  
 264 et al., 2021). The improved parameterization, (3), allows the dependence of the melt rate  
 265 on the entrainment coefficient, clearly shown for the first time in this paper, to be eas-  
 266 ily included in numerical models. As such the true effect of subglacial plumes, includ-  
 267 ing the effects of suspended sediment and geometric effects, on the melting of marine ter-  
 268 minating glaciers can be modelled.

## 269 5 Conclusion

270 Novel laboratory experiments have shown, for the first time, that submarine melt-  
 271 ing of marine-terminating glaciers can be enhanced by up to 60% by the presence of sed-  
 272 iment in a subglacial discharge plume. The experiments have also shown a direct link  
 273 between entrainment into a turbulent plume rising next to an ice face and the melt rate  
 274 of that ice face. In addition to the effect of suspended sediment, this link implies that  
 275 other plume properties that affect the rate of entrainment, such as the source geometry,  
 276 will also affect the melt rate of the ice face.

277 To account for these differences, we propose that the entrainment coefficient of a  
 278 turbulent plume be explicitly included in parameterisations of submarine ice melting (the  
 279 three-equation model). This can be done by redefining the turbulent transfer coefficient  
 280 so that it doesn't (implicitly) include the entrainment coefficient of the plume. Doing  
 281 so would not require any additional parameters in most numerical models, as the entrain-  
 282 ment coefficient is already used to determine the flow velocity next to the ice face. Nonethe-  
 283 less, it would clarify the important processes driving ice melting and facilitate improved  
 284 accuracy of such models.

## 285 6 Open Research

286 Unprocessed experimental parameters and measurements for the ice melting ex-  
 287 periments are provided in the Supplementary Information. Measurements of the entrain-  
 288 ment coefficient in Figure 3 are taken from McConnochie et al. (2021).

289 **Acknowledgments**

290 We gratefully acknowledge technical assistance from Anders Jensen. CDM thanks the  
 291 Weston Howard Jr. Scholarship for funding. Support to CC was given by NSF project  
 292 OCE-1434041 and OCE-1658079.

293 **References**

- 294 Cenedese, C., & Gatto, V. M. (2016). Impact of Two Plumes' Interaction on Subma-  
 295 rine Melting of Tidewater Glaciers: A Laboratory Study. *J. Phys. Oceanogr.*,  
 296 46, 361–367. doi: 10.1175/JPO-D-15-0171.1
- 297 Cenedese, C., & Linden, P. F. (2014). Entrainment in two coalescing axisymmetric  
 298 turbulent plumes. *J. Fluid Mech.*, 752, R2. doi: 10.1017/jfm.2014.389
- 299 Fried, M. J., Catania, G. A., Bartholomaus, T. C., Duncan, D., Davis, M., Stearns,  
 300 L. A., . . . Sutherland, D. (2015). Distributed subglacial discharge drives sig-  
 301 nificant submarine melt at a Greenland tidewater glacier. *Geophys. Res. Lett.*,  
 302 42, 9328–9336. doi: 10.1002/2015GL065806
- 303 Jenkins, A. (2011). Convection-Driven Melting near the Grounding Lines of Ice  
 304 Shelves and Tidewater Glaciers. *J. Phys. Oceanogr.*, 41, 2279–2294. doi: 10  
 305 .1175/JPO-D-11-03.1
- 306 Josberger, E. G. (1980). The effect of bubbles released from a melting ice wall on  
 307 the melt-driven convection in salt water. *J. Phys. Oceanogr.*, 10, 474-477. doi:  
 308 10.1175/1520-0485
- 309 Kaye, N. B., & Linden, P. F. (2004). Coalescing axisymmetric turbulent plumes. *J.*  
 310 *Fluid Mech.*, 502, 41–63. doi: 10.1017/S0022112003007250
- 311 Kerr, R. C., & McConnochie, C. D. (2015). Dissolution of a vertical solid surface  
 312 by turbulent compositional convection. *J. Fluid Mech.*, 765, 211–228. doi: 10  
 313 .1017/jfm.2014.722
- 314 Mankoff, K. D., Straneo, F., Cenedese, C., Das, S. B., Richards, C. G., & Singh,  
 315 H. (2016). Structure and dynamics of a subglacial discharge plume in  
 316 a Greenlandic fjord. *J. Geophys. Res. Oceans*, 121, 8670–8688. doi:  
 317 10.1002/2016JC011764
- 318 McConnochie, C. D., Cenedese, C., & McElwaine, J. N. (2021). Entrainment into  
 319 particle-laden turbulent plumes. *Phys. Rev. Fluids*, 6, 123502. doi: 10.1103/  
 320 PhysRevFluids.6.123502

- 321 McConnochie, C. D., & Kerr, R. C. (2017a). Enhanced ablation of a vertical ice face  
322 due to an external freshwater plume. *J. Fluid Mech.*, *810*, 429–447. doi: 10  
323 .1017/jfm.2016.761
- 324 McConnochie, C. D., & Kerr, R. C. (2017b). Testing a common ice-ocean param-  
325 eterization with laboratory experiments. *J. Geophys. Res. Oceans*, *122*, 5905–  
326 5915. doi: 10.1002/2017JC012918
- 327 Mingotti, N., & Woods, A. W. (2019). Multiphase plumes in a stratified ambient. *J.*  
328 *Fluid Mech.*, *869*, 292–312. doi: 10.1017/jfm.2019.198
- 329 Morton, B. R., Taylor, G. I., & Turner, J. S. (1956). Turbulent gravitational con-  
330 vection from maintained and instantaneous sources. In *Proceedings of the*  
331 *royal society a: Mathematical, physical and engineering sciences* (Vol. 234, pp.  
332 1–23).
- 333 Nienow, P. W. (2017). Recent Advances in Our Understanding of the Role of Melt-  
334 water in the Greenland Ice Sheet System. *Curr. Clim. Change Rep.*, *3*, 330–  
335 344. doi: 10.1007/s40641-017-0083-9
- 336 Pritchard, H. D., Arthern, R. J., Vaughan, D. G., & Edwards, L. A. (2009). Ex-  
337 tensive dynamic thinning on the margins of the Greenland and Antarctic ice  
338 sheets. *Nature*, *461*, 971–975. doi: 10.1038/nature08471
- 339 Richardson, J., & Hunt, G. R. (2022). What is the entrainment coefficient of a pure  
340 turbulent line plume? *J. Fluid Mech.*, *934*, A11. doi: 10.1017/jfm.2021.1070
- 341 Rignot, E., Jacobs, S., Mouginot, J., & Scheuchl, B. (2013). Ice shelf melting around  
342 Antarctica. *Science*, *341*, 266–270. doi: 10.1126/science.1235798
- 343 Slater, D. A., Nienow, P. W., Cowton, T. R., Goldberg, D. N., & Sole, A. J. (2015).  
344 Effect of near terminus subglacial hydrology on tidewater glacier submarine  
345 melt rates. *Geophys. Res. Lett.*, *42*, 2861–2868. doi: 10.1002/2014GL062494
- 346 Straneo, F., & Cenedese, C. (2015). The dynamics of Greenland’s glacial fjords and  
347 their role in climate. *Annu. Rev. Mar. Sci.*, *7*, 89–112. doi: 10.1146/annurev  
348 -marine-010213-135133
- 349 Sutherland, B. R., Rosevear, M. G., & Cenedese, C. (2020). Laboratory ex-  
350 periments modeling the transport and deposition of sediments by glacial  
351 plumes rising under an ice shelf. *Phys. Rev. Fluids*, *5*(1), 13802. doi:  
352 10.1103/PhysRevFluids.5.013802
- 353 Wells, A. J., & Worster, M. G. (2008). A geophysical-scale model of vertical natu-

354 ral convection boundary layers. *J. Fluid Mech.*, 609, 111–137. doi: 10.1017/jfm  
355 .2021.1070